Calhoun: The NPS Institutional Archive

DSpace Repository

Theses and Dissertations 1. Thesis and Dissertation Collection, all items

1999-06

Numerical calculation of the Wannier Functions GaAs/Al(0.25)Ga(0.75)As superlattice structure

Yuvanc, Mustafa.

Monterey, California: Naval Postgraduate School

http://hdl.handle.net/10945/13570

Downloaded from NPS Archive: Calhoun

Calhoun is the Naval Postgraduate School's public access digital repository for research materials and institutional publications created by the NPS community. Calhoun is named for Professor of Mathematics Guy K. Calhoun, NPS's first appointed -- and published -- scholarly author.

Dudley Knox Library / Naval Postgraduate School
411 Dyer Road / 1 University Circle
Monterey, California USA 93943

http://www.nps.edu/library

NAVAL POSTGRADUATE SCHOOL
Monterey, California

THESIS

NUMERICAL CALCULATION OF THE WANNNIER FUNCTIONS OF GaAs/$Al_{0.25}Ga_{0.75}As$ SUPERLATTICE STRUCTURE

by

Mustafa Yuvanc

June 1999

Thesis Advisor:	James H. Luscombe
Co-Advisor	Robert L. Armstead

Approved for public release; distribution is unlimited.

DTIC QUALITY INSPECTED 4

19990708 164

REPORT DOCUMENTATION PAGE

Form Approved OMB No. 0704-0188

Public reporting burden for this collection of information is estimated to average 1 hour per response, including the time for reviewing instruction, searching existing data sources, gathering and maintaining the data needed, and completing and reviewing the collection of information. Send comments regarding this burden estimate or any other aspect of this collection of information, including suggestions for reducing this burden, to Washington headquarters Services, Directorate for Information Operations and Reports, 1215 Jefferson Davis Highway, Suite 1204, Arlington, VA 22202-4302, and to the Office of Management and Budget, Paperwork Reduction Project (0704-0188) Washington DC 20503.

1. AGENCY USE ONLY ***(Leave blank)***

2. REPORT DATE June 1999

3. REPORT TYPE AND DATES COVERED Master's Thesis

4. TITLE AND SUBTITLE Numerical Calculation of the Wannier functions of GaAs/$Al_{0.25}Ga_{0.75}As$ Superlattice Structure

5. FUNDING NUMBERS

6. AUTHOR(S) Yuvanc, Mustafa

7. PERFORMING ORGANIZATION NAME(S) AND ADDRESS(ES)
Naval Postgraduate School Monterey, CA 93943-5000

8. PERFORMING ORGANIZATION REPORT NUMBER

9. SPONSORING / MONITORING AGENCY NAME(S) AND ADDRESS(ES)

10. SPONSORING/MONITORING AGENCY REPORT NUMBER

11. SUPPLEMENTARY NOTES The views expressed in this thesis are those of the author and do not reflect the official policy or position of the Department of Defense or the U.S. Government.

12a. DISTRIBUTION / AVAILABILITY STATEMENT
Approved for public release; distribution is unlimited.

12b. DISTRIBUTION CODE

13. ABSTRACT ***(maximum 200 words)***

This paper presents the numerical calculation of the Wannier functions ($a_n(z)$) of the GaAs/$Al_{0.25}Ga_{0.75}As$ superlattice structure. The Wannier functions are linear combinations of the Bloch functions ($\psi_{nk}(z)$) that can be viewed as a convenient mathematical instrument to get around the lack of orthogonality of the tight binding formulation and are useful tool when the position of an electron has physical importance. However, except for finding a variational principal for the energy levels of one dimensional crystals in terms of the Wannier functions and simple cubic lattice calculations for instructional reasons, models have not been calculated or plotted showing the theory can be expanded to more complex superlattice structures. We develop an algorithm to numerically calculate and plot the Wannier functions of the GaAs/$Al_{0.25}Ga_{0.75}As$ superlattice structure and hence prove that these functions can be calculated even for complex structures. By using the plots of our numerical modelling, we displayed the peculiar properties of the Wannier functions:

a. Wannier functions are real.
b. They fall off exponentially.
c. They are either symmetric or anti-symmetric about $z=0$.

14. SUBJECT TERMS
Wannier functions, superlattice structure, Bloch functions

15. NUMBER OF PAGES 51

16. PRICE CODE

17. SECURITY CLASSIFICATION OF REPORT Unclassified

18. SECURITY CLASSIFICATION OF THIS PAGE Unclassified

19. SECURITY CLASSIFICATION OF ABSTRACT Unclassified

20. LIMITATION OF ABSTRACT UL

Approved for public release; distribution is unlimited

NUMERICAL CALCULATION OF THE WANNIER FUNCTIONS OF GaAs/$Al_{0.25}Ga_{0.75}$As SUPERLATTICE STRUCTURE

Mustafa Yuvanc
1st Lieutenant, Turkish Army
B.S., Turkish Military Academy, 1991

Submitted in partial fulfillment of the
requirements for the degree of

MASTER OF SCIENCE IN PHYSICS

from the

NAVAL POSTGRADUATE SCHOOL
June 1999

Author: [redacted]
Mustafa Yuvanc

Approved by: [redacted]
James H. Luscombe, Thesis Advisor

[redacted]
Robert L. Armstead, Co-Advisor

[redacted]
Department of Physics

ABSTRACT

This paper presents the numerical calculation of the Wannier functions (*$a_n(z)$*) of the GaAs/$Al_{0.25}Ga_{0.75}As$ superlattice structure. The Wannier functions are linear combinations of the Bloch functions ($\psi_{nk}(z)$) that can be viewed as a convenient mathematical instrument to get around the lack of orthogonality of the tight binding formulation and are useful tool when the position of an electron has physical importance. However, except for finding a variational principal for the energy levels of one dimensional crystals in terms of The Wannier functions and simple cubic lattice calculations for instructional reasons, models have not been calculated or plotted showing the theory can be expanded to more complex superlattice structures. We develop an algorithm to calculate numerically and plot the Wannier functions of the GaAs/$Al_{0.25}Ga_{0.75}As$ superlattice structure and hence prove that these functions can be calculated even for complex structures. By using the plots of our numerical modelling, we displayed the peculiar properties of the Wannier functions:

a. Wannier functions are real.

b. They fall off exponentially.

c. They are either symmetric or anti-symmetric about $z=0$.

TABLE OF CONTENTS

I. INTRODUCTION 1

II. THE WANNIER FUNCTIONS AND THEIR PROPERTIES 3

III. SUPERLATTICE EFFECTIVE-MASS SCHRODINGER EQUATION 7

IV. THE WANNIER FUNCTIONS IN FINITE DIFFERENCE FORM 13

V. RESULTS AND CONCLUSIONS 17

A. BANDSTRUCTURE FUNCTION 17

B. WANNIER FUNCTIONS 19

C. CONCLUSION AND FINAL REMARKS 24

APPENDIX A: COMPUTER CODE IN MATLAB PROGRAMMING LANGUAGE FOR NUMERICAL CALCULATION OF THE BANDSTRUCTURE FUNCTION 29

APPENDIX B: COMPUTER CODE IN MATLAB PROGRAMMING LANGUAGE FOR NUMERICAL CALCULATION OF THE WANNIER FUNCTIONS 33

LIST OF REFERENCES 37

INITIAL DISTRIBUTION LIST 39

ACKNOWLEDGEMENT

First of all, I would like to thank my advisor Prof. J. H. Luscombe who made this lifetime goal come true. Secondly, I would like to express my gratitude to Prof. R. L. Armstead for his support.

I would like to dedicate this thesis to my family, my wife Birgul and my son Egem, without whom this goal cannot be achieved. She has showed me that the biggest input to success is a loving family.

And finally I want to thank my good friend Scott Bewley (USN) and his wife Lorelle who showed me what a good friendship is and who helped me and supported me in all phases of this thesis.

I. INTRODUCTION

Semiconductor superlattices are a novel class of man-made solids which consist of a repetition of alternating layers of two or more different semiconductor materials. By adding artificial periodicity to the multi-layered structure [Ref. 1], the electronic nature of the superlattice can be controlled through the constituent material's crystalline orientation, layer thickness and material composition. The result of this periodic layering process creates semiconductor superlattices which present exciting optical and electronic characteristics which cannot be found in existing semiconductor crystals [Ref. 2].

From the beginning of the study of this new class of solids, most of the attention and research has been concentrated on new generations of optoelectronic device applications. One of the promising device implementations is fast and highly sensitive InAlGaAs/InAlAs superlattice avalanche photodiodes for use in 1.3 to 1.6 μm optical communications [Ref. 3]. Other areas of research include the study of superlattices for the future generation of far infrared detector imaging arrays with wavelength $\lambda>12$ μm [Ref. 4] and the study of high optical confinement effects [Ref. 5] leading to investigations of using superlattices to reduce the threshold current density and enhance the device stability of semiconductor lasers.

Even though successful device implementations have been reported, and a world-wide research effort is underway in this new field of study, many problems remain unsolved. These problems include everything from the preparation of the superlattices to understanding the transport and optical phenomena introduced by these novel materials.

In this thesis, the Wannier functions ($a_n\ (z-d_j)$) of a GaAs/$Ga_{0.75}Al_{0.25}As$ superlattice is numerically calculated and plotted with the new lattice constant in the growth direction z set by d_{GaAs}+d_{AlGaAs} (Fig. 1). The Wannier functions can be viewed as

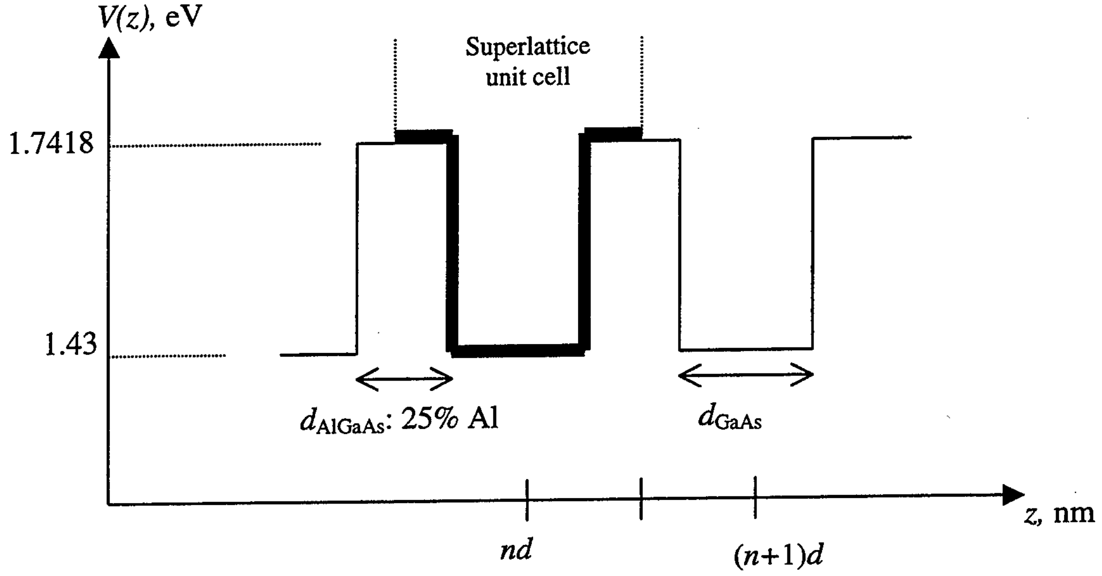

Figure 1: Conduction band edge profile of GaAs/$Al_{0.75}Ga_{0.25}As$ superlattice with the new lattice constant $d = d_{AlGaAs} + d_{GaAs}$ where d_{AlGaAs} and d_{GaAs} are are thickness of the corresponding semiconductors.

a convenient mathematical instrument to get around the lack of orthogonality of the tight-binding formulation . It is also a useful tool in understanding the spatially localized nature of electrons when they are near an impurity state. Except for theoretical studies on finding a variational principal for the energy levels of one dimensional crystals in terms of the Wannier functions [Ref. 6], and simple cubic lattice calculations for instructional reasons [Ref. 7], models have not yet been calculated or plotted showing the theory can be expanded to more complex superlattice designs. This thesis will numerically calculate and plot the Wannier functions of GaAs/$Al_{0.25}$ $Ga_{0.75}$ As superlattice structure to prove the theory beyond the simple cubic problem and will display the properties of these functions graphically.

II. THE WANNIER FUNCTIONS AND THEIR PROPERTIES

In a one dimensional crystal, the mathematical basis for the motion of an electron can be expressed by the Schrodinger equation as

$$\left[-\frac{\hbar^2}{2m}\frac{d^2}{dz^2}+V(z+c)\right]\psi = E\psi \tag{1}$$

where $V(z)$ is a periodic potential function of the crystal in the growth direction z with the period of lattice constant c, i.e., $V(z)=V(z+c)$ and m is the mass of the electron. Bloch has shown that the eigenfunctions of the one-electron Schrodinger equation, or Bloch states, for this periodic potential (Eqn. 1) have the mathematical form [Ref. 8]

$$\psi_{nk}(z) = e^{ikz}u_{nk}(z) \tag{2}$$

where $u_{\mathrm{nk}}(z)$ is a function with the periodicity of the potential. The subscript n stands for the n^{th} energy band to which the eigenfunctions belong and the subscript k is the wave vector in the growth direction z.

In the method of the tight binding formulation, using atomic wave functions as a basis set has a practical advantage over Bloch states in qualitative calculations [Ref. 9]. The actual calculations with those functions, however, create difficulties due to the atomic wave functions being centered on different atomic sites that are not orthogonal to each other. Furthermore, they are not necessarily orthogonal for different k values either.

Wannier has introduced a set of localized wave functions, $a_n(z-c_j)$, which are linear combinations of all the Bloch states $\psi_{nk}(z)$ for a given energy band, and have the advantages of orthogonality [Ref. 10]:

$$a_n(z-c_j) = \frac{1}{\sqrt{N}}\sum_k e^{-ikc_j}\psi_{nk}(z) \tag{3}$$

where

$$a_n(z) = \frac{1}{\sqrt{N}} \sum_k \psi_{nk}(z) \tag{4}$$

N is the number of lattice sites in the one dimensional crystal and subscript *j* stands for the lattice site of which we are going to calculate the Wannier function. The summation in Equation 4 extends over all values of the first Brillouin zone (BZ). The Bloch function $\psi_{nk}(z)$ is continuous in *k*, and is the same function of *k* at *k*+*K* where *K* is a reciprocal lattice vector, i.e., the Bloch functions are periodic in the reciprocal lattice [Ref. 11]. Since the Wannier functions are functions of distance from the direct lattice site *j*, we may think of Equation 3 and 4, i.e., $\psi_{nk}(z)$ and $a_n(z-c_j)$ as the Fourier transform of each other. The Fourier-transform of Equation 3 defining the Wannier functions, can now be calculated to obtain the Bloch functions:

$$\psi_{nk}(z) = \frac{1}{\sqrt{N}} \sum_j e^{ikc_j} a_n(z - c_j) \tag{5}$$

The Wannier functions can show orthonormality properties in contrast to the tight binding formulation, because the Wannier functions centered on different lattice site and/or or belonging to different energy bands are orthogonal to each other :

$$\begin{aligned}\int a_n^*(z-c_j)a_m(z-c_i)dz &= \frac{1}{\sqrt{N}} \sum_{k,k'} e^{ikc_j} e^{-ikc_i} \int \psi_{nk}^*(z)\psi_{mk'}(z)dz \\ &= \frac{1}{N} \sum_{k,k'} e^{i(kc_j - k'c_i)} \delta_{nm} \delta_{kk'} \\ &= \delta_{nm} \delta_{c_i c_j} \end{aligned} \tag{6}$$

where we have invoked the summation relation

$$\sum_k e^{ik(c_i-c_j)} = N\delta_{c_ic_j} \tag{7}$$

and the orthogonality of the Bloch functions. Hence, the Wannier functions form a complete orthonormal set, and the completeness can be shown by summing over all

energy bands and all lattice sites,

$$\sum_{n,j} a_n^*(z-c_j)a_n(z'-c_j) = \delta(z-z'). \tag{8}$$

For a one dimensional periodic potential with no degeneracies of energy bands, It has been rigorously shown that the Wannier functions will decay exponentially at large distances [Ref. 12]. For our purposes, we can easily show this localized nature of the Wannier functions qualitatively. If we replace z with c_i in Equation 3 where c_i is a lattice vector, then we get

$$a_n(c_i-c_j) = \frac{1}{\sqrt{N}}\sum_k e^{-ik(c_i-c_j)}\psi_{nk}(z) \tag{9}$$

When $|\, c_i - c_j \,|$ becomes large the exponential part of the summation oscillates rapidly and contributes vanishingly to the summation. Hence, we can expect the Wannier functions of one energy band to fall off exponentially at large distances and to be identical functions which are centered at each of the lattice points.

One of the most interesting properties of the Wannier functions is their reality. Regardless of the phases of the Bloch functions, Wannier functions are real. W. Kohn has discussed the reality problem of the Wannier functions in detail [Ref.12]. We are not going to prove this peculiar aspect of the Wannier functions in this paper, but we refer the reader to W. Kohn's paper.

With the aforementioned properties, the Wannier functions can be considered a useful mathematical tool when the position of an electron has physical importance, e.g., in the discussion of the motion of an electron around an impurity site. Other important areas of application include deriving a transport theory for Bloch electrons [Ref. 13]. Also, using Wannier functions in the calculation of energy bands has been discussed but no practical application emerged [Ref. 14].

III. SUPERLATTICE EFFECTIVE-MASS SCHRODINGER EQUATION

Before presenting our method of numerical calculation of the Wannier functions, we are going to derive the Schrodinger equation for the GaAs/$Al_{0.75}Ga_{0.25}As$ superlatice structure (Fig. 1) by using the effective mass theory with the Kronig-Penney model. This approach describes the electron with an effective mass m_i^* where subscript *i* corresponds to the constituent layers of the superlattice, and approximates the superimposed perturbing potential (Superlattice bandedge profile) as periodic square wells (Fig. 1).

If H is the Hamiltonian for an electron in a one dimensional perfect crystal, then

$$H\psi_{nk}(z) = E_n(k)\psi_{nk}(z) \qquad (10)$$

where

$$H = -\frac{\hbar^2}{2m}\frac{\partial^2}{\partial z^2} + V(z), \qquad (11)$$

and $E_n(k)$ are the eigenvalues of the Bloch functions $\psi_{nk}(z)$, namely the band structure function. Since band structure function $E_n(k)$ is a non-degenerate and continuous function of *k* with the periodicity of the crystal in the reciprocal space (*k*-space) [Ref. 15], we have the possibility of defining the Fourier expansion of it as we did for the Bloch functions (Eqn. 5):

$$E_n(k) = \sum_c E_n(c)e^{ick} \quad . \qquad (12)$$

where the summation is over the lattice sites of the host material in the growth direction (*z*), and $E_n(c)$ is the Fourier expansion coefficient.

Since the band structure function $E_n(k)$ is an analytic function of k and the wave functions $\psi_{nk}(z)$ have the periodicity of the crystal, we can assume the replacement of the perfect crystal Hamiltonion (*H*) by the operator $E_n(-i\frac{\partial}{\partial z})$ which follows from $E_n(k)$ when Hermitian differential operator $-i\frac{\partial}{\partial z}$ is used in place of *k* [Ref. 16] where *i* is $\sqrt{-1}$. We will show that *H* and $E_n(-i\frac{\partial}{\partial z})$ have the same eigenvalues and eigenfunctions. From Equation 10, we have

$$E_n(-i\frac{\partial}{\partial z})\psi_{nk}(z) = \sum_c E_n(c)e^{c\frac{\partial}{\partial z}}\psi_{nk}(z)$$

$$= \sum_c E_n(c)\left(1 + c\frac{\partial}{\partial z} + \frac{1}{2}(c\frac{\partial}{\partial z})^2 + \ldots\right)\psi_{nk}(z)$$

$$= \sum_c E_n(c)\left(\psi_{nk}(z) + c\frac{\partial}{\partial z}\psi_{nk}(z) + \frac{1}{2}c^2\frac{\partial^2}{\partial z^2}\psi_{nk}(z) + \ldots\right).$$

The term on the right hand side in the brackets is nothing but the Taylor expansion of the Bloch function $\psi_{nk}(z+c)$. Therefore, we obtain

$$E(-i\frac{\partial}{\partial z})\psi_{nk}(z) = \sum_c E_n(c)\psi_{nk}(z+c)$$

$$= \sum_c E_n(c)e^{ick}\psi_{nk}(z)$$

$$= E_n(k)\psi_{nk}(z) \quad . \tag{13}$$

We have used the Fourier transform of the band structure function (Eqn. 12) and Bloch's theorem [Ref. 17]:

$$\psi_{nk}(z \pm c) = e^{\pm ikc}\psi_{nk}(z) \quad . \tag{14}$$

As can be noted, the periodic potential of the crystal structure *V(z)* in Equation 11 is not explicitly present in this formulation (Eqn. 13) where it is incorporated with the usual kinetic energy operator,

$$-\frac{\hbar^2}{2m}\frac{\partial^2}{\partial z^2} \quad . \tag{15}$$

The unperturbed Hamiltonian defined by the modified kinetic energy operator $E(-i\frac{\partial}{\partial z})$ would be far more complicated than the kinetic energy operator $-\frac{\hbar^2}{2m}\frac{\partial^2}{\partial z^2}$, if we tried to include the full *k*-dependence of the band structure function $E_n(k)$ [Ref. 18]. However, many aspects of the electronic properties of semiconductors can be obtained from a small number of excited electrons found at the bottom of the conduction band and holes created in the absence of these electrons at the top of the valence band. Hence, what we need is the form of the band structure function for these carriers over a small region of *k*-space around the band extrema. This implies that the bandstructure function can generally be drawn as a quadratic function of *k*. Besides, for most of the semiconductors, $E_n(k)$ is approximately parabolic near an extremum, as for the conduction band edge of GaAs and $Al_{0.75}Ga_{0.25}As$ [Ref. 19]. For the present problem, by restricting our treatment to the band extremum E_o occuring around the wave vector value $k = k_0 = 0$ which is the case for direct gap semiconductors like GaAs, we take the Taylor series expansion of $E_n(k)$:

$$E_n(k) = E_0 + \beta_1(k-k_0) + \frac{1}{2}\beta_2(k-k_0)^2 + \ldots\ldots \tag{16}$$

where the expansion coefficients are

$$\beta_i = \left(\frac{\partial^i E}{\partial k^i} \right)_{k=k_0} \quad , \tag{17}$$

the subscript *i* representing the order of expansion. Since the Taylor expansion of E-k relation around the band extremum is relevant to the problem, the first order term $\beta_1(k-k_0)$ will vanish by construction, and higher order tems can be neglected. For dimensional reasons, β_2 must have the units of $\hbar^2/m$. Therefore, by defining an effective mass (m^*) of the electron and replacing the curvature of the E-k relation with $\hbar^2/2m^*$, the band structure function near the extremum point can be characterized as

$$E_n(k) = E_0 + \frac{\hbar^2}{2m^*}k^2 \quad . \tag{18}$$

Once again, by replacing the canonical substitution $-i\frac{\partial}{\partial z}$ in place of *k* in Equation 18, we obtain the effective mass Schrodinger equation for a bulk crystal,

$$\left[\frac{-\hbar^2}{2m^*}\frac{\partial^2}{\partial z^2} + E_0 \right] \psi_{nk}(z) = E_n(k)\psi_{nk}(z) \quad , \tag{19}$$

where the effect of the crystal potential *V(z)* is absorbed in the parameter m^*.

Now that the Schrodinger equation for the perfect crystal has been formulated, we can introduce our perturbing potential $U_s(z)$ shaped by the GaAs/$Al_{0.25}Ga_{0.75}As$ superlattice in the growth direction *z*. By applying the Kronig-Penney model depicted earlier, the superimposed superlattice potential can be expressed as

$$\begin{aligned} U_s(z) &= E_c^{AlGaAs} - E_c^{GaAs} = \Delta E_c \qquad && |z - nd| \rangle d_{GaAs}/2 \\ &= 0 && |z - nd| \langle d_{GaAs}/2 \quad , \end{aligned} \tag{20}$$

where E_c^{GaAs} and E_c^{AlGaAs} are the bottom of the conduction bands of GaAs and $Al_{0.25}Ga_{0.75}As$ respectively and *d* is the superlattice constant defined earlier. Equation 20 explicitly implies that $U_s(z)$ is a periodic function of *z* with the periodicity *d*, i.e.,

$$U_s(z) = U_s(z+nd) \quad . \tag{21}$$

By defining the perturbing superlattice periodic potential $U_s(z)$, which is superposed over the intrinsic crystal potential of the host material, the Schrodinger equation for $GaAs/Al_{0.25}Ga_{0.75}As$ superlattice can be then written as

$$\left[-\frac{\hbar^2}{2m^*(z)}\frac{\partial^2}{\partial z^2}+U_s(z)\right]\psi_{nk}(z)=\varepsilon_n(k)\psi_{nk}(z) \ , \tag{22}$$

where we moved E_0 to the right-hand side of the Equation 22 and defined $\varepsilon_n(k)$ which is the difference between bandstructure function $E_n(k)$ and band extremum E_0. This rearranging of energy terms will give the energy values from the edge of the conduction band of the constituent layer (Since $E_c^{GaAs} < E_c^{AlGaAs}$, in this context it is GaAs) which is approximated as a quantum well by the Kronig-Penney model. The spatial dependence on the growth direction *z* is brought in to the effective mass $(m^*(z))$ since the materials forming the layers of the superlattice have different values of effective mass.

Since the Bloch functions are orthogonal for different energy values which are real, it requires the hermiticity of the Hamiltonian (Energy operator),

$$H = -\frac{\hbar^2}{2m^*(z)}\frac{\partial^2}{\partial z^2}+U_s(z) \quad . \tag{23}$$

But, this form of the Hamiltonian is not accurate when the effective mass has spatial dependence , since the canonical operator $-i\frac{\partial}{\partial z}$ does not commute with *z*, which requires the correct ordering of $-i\frac{\partial}{\partial z}$ and $\frac{1}{m^*(z)}$ terms. For example, let us consider an interface between the two constituent layers (GaAs and Al$_{0.25}$Ga$_{0.75}$As), say at z_0. The wave function $\psi_{nk}(z)$ has to obey the usual boundary conditions [Ref. 20] to guarantee current conservation across the junction,

$$\psi_{nk}(z_0^{GaAs}) = \psi_{nk}(z_0^{AlGaAs}) \tag{24}$$

$$\left.\frac{\partial \psi_{nk}(z)}{\partial z}\right|_{z_0^{GaAs}} = \left.\frac{\partial \psi_{nk}(z)}{\partial z}\right|_{z_0^{AlGaAs}} \quad , \tag{25}$$

where z_0^{GaAs} and z_0^{AlGaAs} are the sides of the junction in GaAs and Al$_{0.25}$Ga$_{0.75}$As layers respectively. On the other hand, the layers have different effective masses [Ref. 21]. So, the boundary condition for matching the derivatives of the wave functions (Eqn. 25) must take the effective masses into account:

$$\left.\frac{1}{m^*_{GaAs}}\frac{\partial \psi_{nk}(z)}{\partial z}\right|_{z_0^{GaAs}} = \left.\frac{1}{m^*_{AlGaAs}}\frac{\partial \psi_{nk}(z)}{\partial z}\right|_{z_0^{AlGaAs}} \tag{26}$$

where m^*_{GaAs} and m^*_{AlGaAs} are effective masses of the electron in the corresponding semiconductors. Since the derivative in Equation 26 is apparently the Hermitian differential operator, the hermiticity here also guarantees the current conservation. As a result of these consideration, the correct form of the Schrodinger equation with a spatially dependent effective mass is given by

$$-\hbar^2\frac{\partial}{\partial z}\frac{1}{m^*(z)}\frac{\partial \psi_{nk}(z)}{\partial z} + U_s(z)\psi_{nk}(z) = E_n(k)\psi_{nk}(z) \ , \tag{27}$$

which assures the hermiticity and guarantees the conservation of current at the interface.

IV. THE WANNIER FUNCTIONS IN FINITE DIFFERENCE FORM

In this chapter we will present the numerical approach which is utilized to obtain the Wannier functions of the GaAs/$Al_{0.25}Ga_{0.75}As$ superlattice structure. The algorithm is then built in two steps: The first step is to solve Equation 27 for the wave functions $\psi_{nk}(z)$ and the eigenvalues $\varepsilon_n(k)$ (Bandstructure function). In the second step we only need to use Equation 4 to calculate and plot the Wannier functions; i.e., for each band index n, we sum the wave functions over all values of k.

We are going to use finite difference approximation [Ref. 22] to solve the superlattice effective mass equation (Eqn. 27) for the wave functions. In this method, we evaluate the values of $\psi_{nk}(z)$ at discrete points z_j which are obtained by dividing the superlattice unit cell into finite number, N-1, of intervals Δz defined by

$$\Delta z = z_{j+1} - z_j \quad . \tag{28}$$

The first derivative in the finite difference form at the point z_j may be written as

$$\frac{\partial}{\partial z}\psi_{nk}(z)\Big|_{z_j} = \frac{\psi_{nk}(z_j + \Delta z) - \psi_{nk}(z_j - \Delta z)}{2\Delta z} \quad . \tag{29}$$

The expression for the second derivative can be obtained by applying Equation 29 successively [Ref. 23]:

$$\frac{\partial}{\partial z}\frac{1}{m^*(z)}\frac{\partial}{\partial z}\psi_{nk}(z)\Bigg|_{z_j} =$$

$$\frac{\frac{1}{m^*(z_{j+1})}\psi_{nk}(z_{j+2}) - \left(\frac{1}{m^*(z_{j+1})} + \frac{1}{m^*(z_{j-1})}\right)\psi_{nk}(z_j) + \frac{1}{m^*(z_{j-1})}\psi_{nk}(z_{j-2})}{(2\Delta z)^2} \tag{30}$$

Before writing the eigenvalue matrix equation for Equation 27, we have to take care of the boundary conditions along the growth direction z. In the artificial periodicity d

of the superlattice, the wave function must satisfy the Bloch theorem (Eqn. 14) [Ref. 17]:

$$\psi_{nk}(z \pm d) = e^{\pm ikd}\psi_{nk}(z) \quad . \tag{14}$$

In the finite difference matrix equation, we replace $\psi_{nk}(z_0)$ and $\psi_{nk}(z_{N+1})$ according to Equation 14. Since we have expressions for each mesh point z_j in the superlattice unit cell, Equation 27 can be rewritten as an eigenvalue equation. By setting $2\Delta z = \omega = d/(N-1)$ and an replacing the constants in Equation 27 with

$$\Gamma_{AlGaAs} = -\frac{\hbar^2}{2m^*_{AlGaAs}\omega^2} = \Gamma_A \qquad \Gamma_{GaAs} = -\frac{\hbar^2}{2m^*_{GaAs}\omega^2} = \Gamma_G$$

$$V_{AlGaAs} = \Delta E_c + \frac{\hbar^2 k^2}{2m^*_{AlGaAs}} = V_A \qquad V_{GaAs} = \frac{\hbar^2 k^2}{2m^*_{GaAs}} = V_G \tag{31}$$

and using Equation 30, we get the eigenvalue matrix equation for each value of k:

$$\begin{bmatrix} -2\Gamma_A + V_A & \Gamma_A & 0 & 0 & 0 & 0 & 0 & 0 & \Gamma_A e^{-ikd} \\ \Gamma_A & -2\Gamma_A + V_A & \Gamma_A & 0 & 0 & 0. & 0 & 0 & 0 \\ 0 & \Gamma_A & \cdot & \cdot & 0 & 0. & 0 & 0 & 0 \\ 0 & 0 & \cdot & \cdot & \Gamma_G & 0 & 0 & 0 & 0 \\ 0 & 0 & 0 & \Gamma_G & -2\Gamma_G + V_G & \Gamma_G & 0 & .0 & 0 \\ 0 & 0 & 0 & 0 & \lambda_G & -2\Gamma_G + V_G & \Gamma_G & 0 & 0 \\ 0 & 0 & 0 & 0 & 0 & \lambda_G & \cdot & \cdot & 0 \\ 0 & 0 & 0 & 0 & 0 & 0. & \cdot & \cdot & \Gamma_A \\ \Gamma_A e^{ikd} & 0 & 0 & 0 & 0 & 0 & 0 & \Gamma_A & -2\Gamma_A + V_A \end{bmatrix} \times$$

$$\begin{bmatrix} \psi_{nk}(z_1) \\ \psi_{nk}(z_2) \\ \cdot \\ \cdot \\ \cdot \\ \cdot \\ \cdot \\ \cdot \\ \psi_{nk}(z_N) \end{bmatrix} = \varepsilon_n(k) \begin{bmatrix} \psi_{nk}(z_1) \\ \psi_{nk}(z) \\ \cdot \\ \cdot \\ \cdot \\ \cdot \\ \cdot \\ \cdot \\ \psi_{nk}(z_N) \end{bmatrix} \quad . \tag{32}$$

Once we have obtained the wave functions for each value of the reciprocal wave vector *k* for a specific band index *n*, we will create a subroutine to sum the wave functions over all the *k* values in the first Brillouine zone (BZ) (Eqn. 4) to calculate and plot the Wannier functions of our superlattice structure.

V. RESULTS AND CONCLUSIONS

The computer codes in the Appendix A and B have been developed for the solution of the effective mass Schrodinger equation for the GaAs/$Al_{0.25}Ga_{0.75}As$ superlattice consisting of, alternately, $Al_{0.25}Ga_{0.75}As$ and GaAs layers. For the purpose of this paper, we have chosen the thickness of the $Al_{0.25}Ga_{0.75}As$ layer as 6 nm and because of our familiarity with it, the Matlab programming language has been used.

A. BANDSTRUCTURE FUNCTION

Before presenting the objective of this paper, i.e., plotting the Wannier functions of the GaAs/$Al_{0.25}Ga_{0.75}As$ superlattice, we wanted to make sure that the eigenvalue matrix equation (Eqn. 32) that we formed as the discretization of the superlattice Schrodinger equation (Eqn. 27) is accurate. The easiest and the most effective way to do so would be to compare the eigenvalues of the matrix equation (Band structure function) to another method (which has already proven itself to be correct) of finding the band structure function of a superlattice structure.

We first created a subroutine in Appendix A for the evaluation of the eigenvalues $\varepsilon_n(k)$ of the matrix equation (Eqn. 32) which gave us the bandstructure function of the superlattice. Next in the second subroutine, we used G. Bastard's analytic superlattice dispersion relation equation [Ref. 24]

$$Cos(kd) = Cos(k_G d_G)Cos(k_A d_A) - \frac{1}{2}\left(\frac{k_A}{k_G} + \frac{k_G}{k_A}\right)Sin(k_G d_G)Sin(k_A d_A) \qquad (33)$$

where

$$k_G = k_{GaAs} = \sqrt{\frac{2\varepsilon_n(k)m^*_{GaAs}}{\hbar^2}} \quad , \quad k_A = k_{AlGaAs} = \sqrt{\Delta E_c + \frac{2\varepsilon_n(k)m^*_{AlGaAs}}{\hbar^2}}$$

$$d_G = d_{GaAs} \quad , \quad d_A = d_{Al;GaAs} \tag{34}$$

to compare with the eigenvalues of the matrix equation. Equation 33 and 34 are implicit equations relating the energy values $\varepsilon_n(k)$ to the wave vector k.

Figure 2 shows the bandstructure function obtained by evaluating the eigenvalues of the matrix equation (Eqn. 32), while Figure 3 is the solution of the Equation 34 satisfying the dispersion relation (Eqn. 33). By inspection, it is clearly seen that the two bandstructure figures are in good agreement with each other. That is to say, the eigenvalue matrix equation formed as the discretization of the superlattice effective-mass Schrodinger equation (Eqn. 27) is accurate.

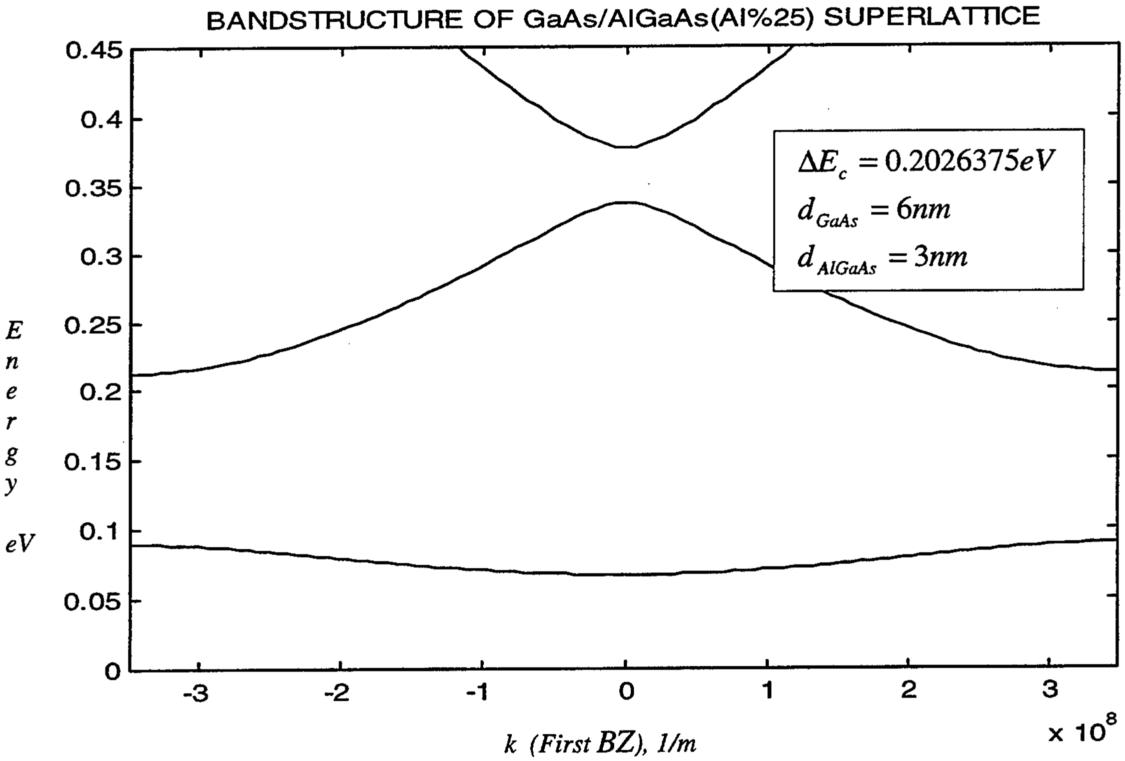

Figure 2: Bandstructure function $\varepsilon_n(k)$ obtained by evaluating the eigenvalues of the matrix equation (Eqn. 32) where $\Delta E_c = E_c^{AlGaAs} - E_c^{GaAs}$.

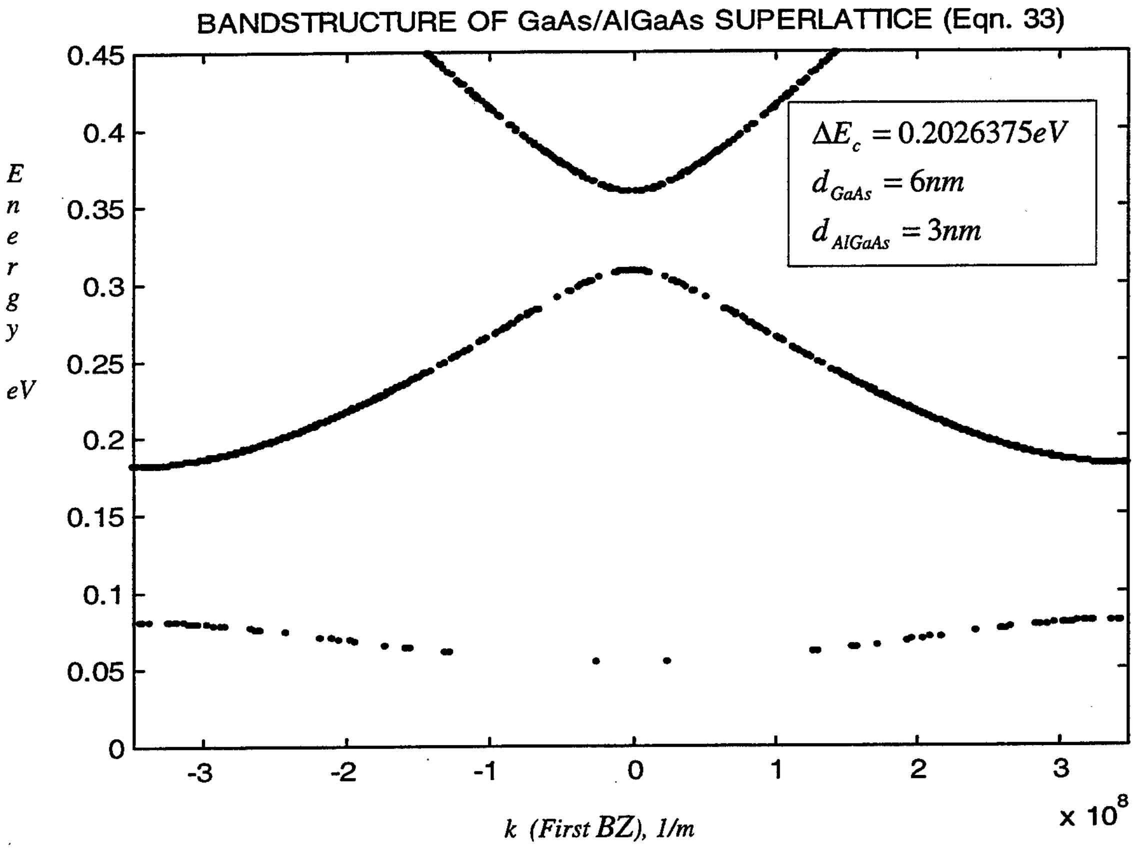

Figure 3: Bandstructure function $\varepsilon_n(k)$ obtained by solving the G. Bastard's superlattice dispersion relation equation (Eqn. 33 and 34) where $\Delta E_c = E_c^{AlGaAs} - E_c^{GaAs}$.

B. WANNIER FUNCTIONS

After confirming the accuracy of the numerical modeling of the superlattice Schrodinger equation (by comparing with the G. Bastard's superlattice dispersion relation), the computer code in Appendix B implements an algorithm which calculates and plots the Wannier functions of the GaAs/$Al_{0.25}Ga_{0.75}As$ superlattice structure. At this phase of our numerical modelling, we deliberately skip the normalization of the Bloch waves. There are three reasons for this: First of all, the Bloch functions can easily be calculated and have been obtained by solving the Schrodinger equation for each value of k and n [Ref. 25]. Secondly, we are not concerned with the normalization of the Bloch functions, since having arbitrary amplitudes for the Wannier functions of any band index (n) is immaterial for the purpose of this paper, i.e., plotting and pointing out the properties of the Wannier functions. The third reason which is the limitation of our modelling is that normalizing each Bloch function of every superlattice unit cell would be formidable to carry out numerically if you discretized 300 mesh points for each superlattice site (z_j) and 100 mesh points in the first BZ (k) which brings out 30,000 Bloch functions just for the first band index (n=1) to deal with. We are going to point out this computational difficulty in the conclusion and final remarks subchapter.

In Chapter II, we have with inclusive detail proved that for each band index (n) there exists only one Wannier function. Since for most of the optical and electronic applications the first two bands of the bandstructure function are utilized, in the computer code (Appendix B) we numerically calculated the Wannier functions of those bands, i.e., n=1 and n=2. Favorably, plotting the Wannier functions for these two bands suffices for the purpose of this paper. Furthermore, we developed the computer code in such a way that by changing the band index entry in the program we can obtain the Wannier functions of any band index that we are interested in.

Figure 4 shows the Wannier function of the first band ($a_1(z)$) extending to the right neighboring superlattice site. By inspection, it is clearly recognized that the Wannier function ($a_1(z)$) is localized and centered at the superlattice site which is shown

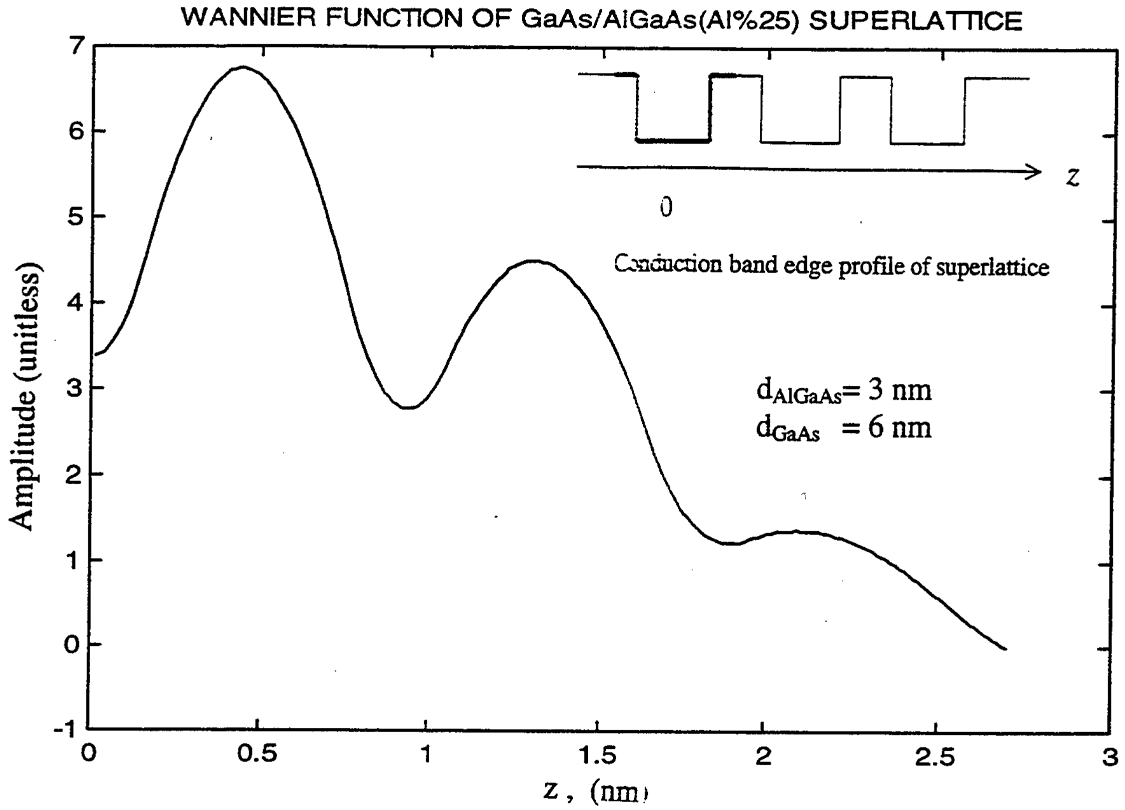

Figure 4 : The Wannier function of GaAs/$Al_{0.25}Ga_{0.75}As$ superlattice for the first band index ($a_1(z)$).

with a thick line in Figure 4. The asymptotic behavior is also observed easily as the Wannier function decays down in the neighboring superlattice unit cell since as $\left|z-d_i\right|$ increases (Eqn. 9), the Bloch functions destroy each other by interference which we had proved thoroughly in Chapter II (See the discussion after Equation 9).

We shall now show that the Wannier functions are real. That is to say, if we tried to plot the imaginary part of the numerically calculated Wannier function of the first band (or any band), we should get an empty figure. However, since the numerical approach (finite difference method) that we used to solve the superlattice Schrodinger equation (Eqn. 27) is just an approximation, we would expect some amplitude as error. Figure 5

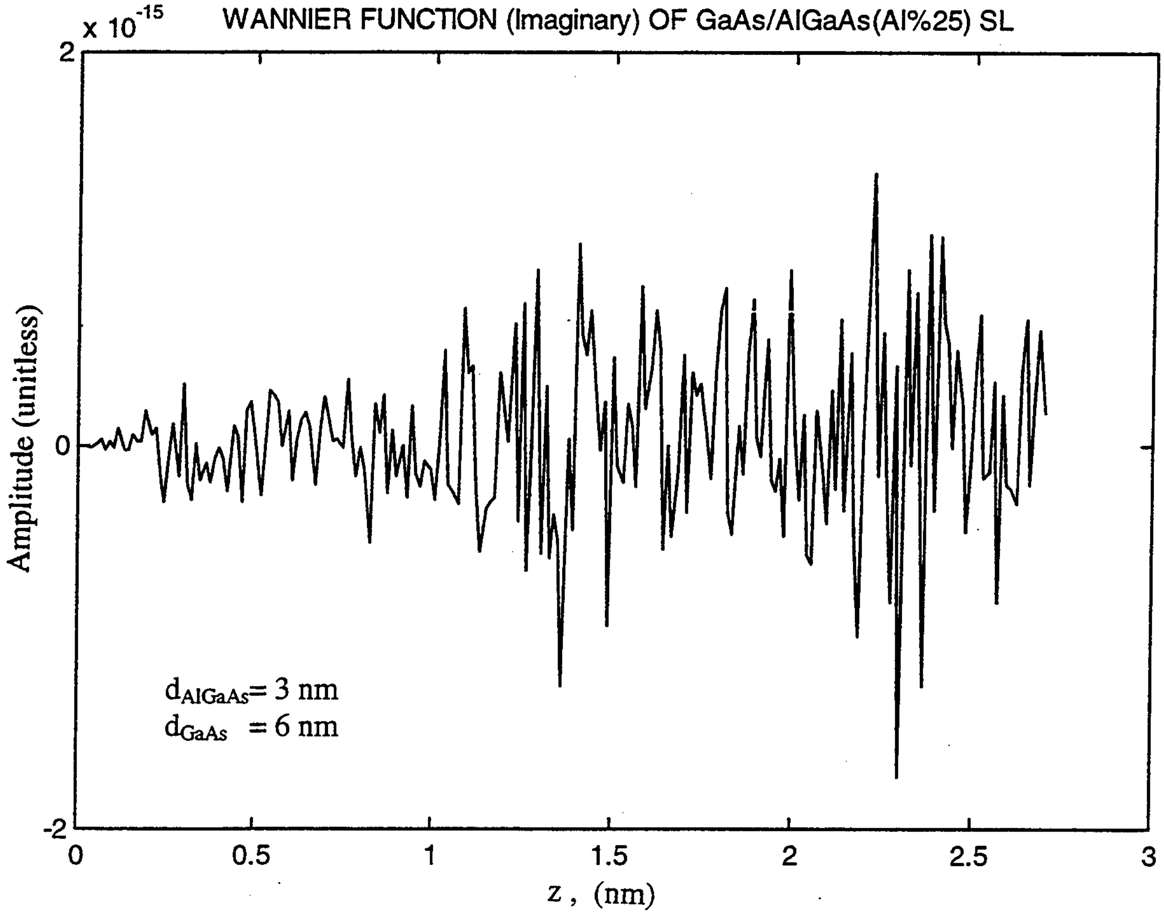

Figure 5: Imaginary part of the numerically calculated Wannier function of GaAs/$Al_{0.25}$ $Ga_{0.75}$ As superlattice for the first band index (*n*=1).

shows the imaginary part of the Wannier function of the first band ($a_1(z)$). Indeed, if we note the order of amplitude which is around 10^{-15}, we can confidently state that the Wannier functions for theGaAs/$Al_{0.25}Ga_{0.75}$As superlattice is real.

Figure 6 depicts the Wannier function of the superlattice (SL) structure for the band index n=2 ($a_2(z)$). The localised nature and the asymptotic behavior are obviously recognized as we did for the $a_1(z)$. Again, the Wannier function $a_2(z)$ is centered at the same superlattice unit cell as we have verified for $a_1(z)$ in Figure 4. The important aspect of Figure 6 is the anti-symmetry of the Wannier function for the band index 2 ($a_2(z)$) about z=0 where we can easily see the symmetry of the Wannier function for the band index n=1($a_1(z)$) in Figure 4. W. Kohn has given a comprehensive discussion about the symmetry properties of the Bloch and the Wannier functions [Ref. 25]. Basically the (anti-) symmetry property of the Wannier functions about z=0 can be accounted for by

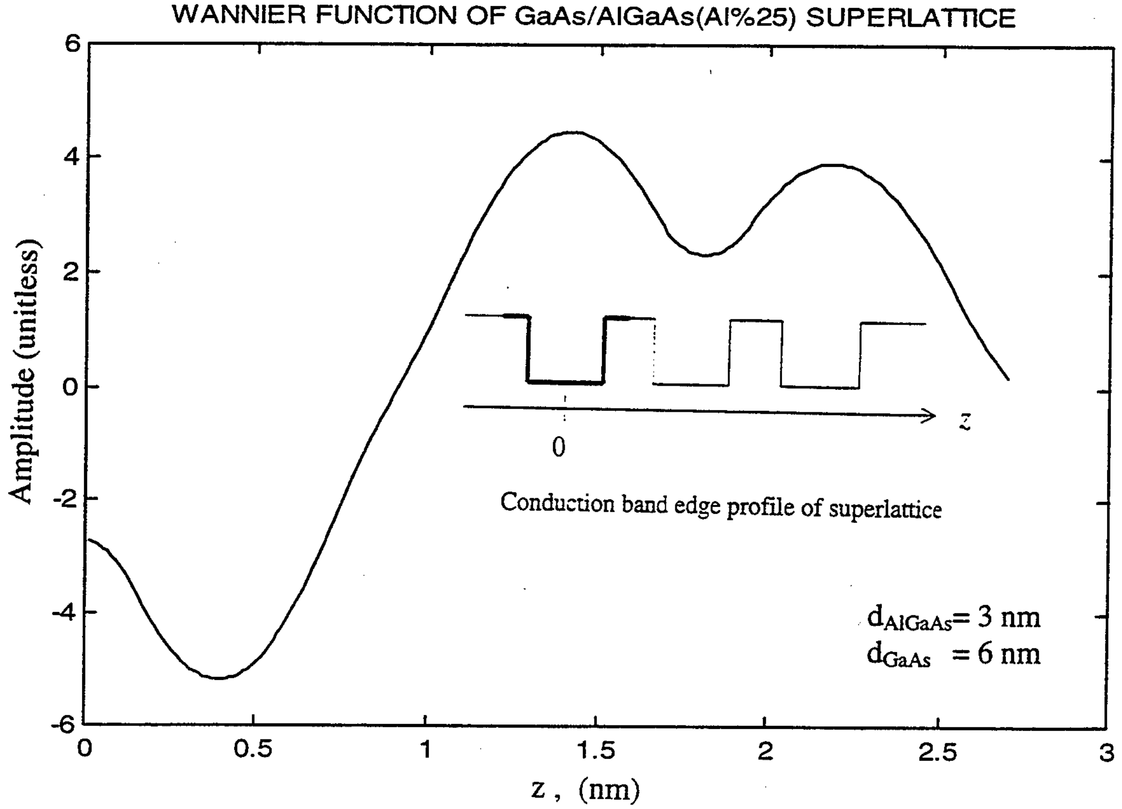

Figure 6: The Wannier function of GaAs/$Al_{0.25}Ga_{0.75}As$ superlattice for the second band index ($a_2(z)$).

the parity of the Bloch functions which could be easily perceived if we revisited the basic quantum mechanics problem of square well.

The reality of the Wannier functions can again be shown if we plot the imaginary part of $a_2(z)$ which is resulted from our numerical approach (Fig. 7). Note the amplitude of the numerically calculated imaginary part of $a_2(z)$ which is around 10^{-15}.

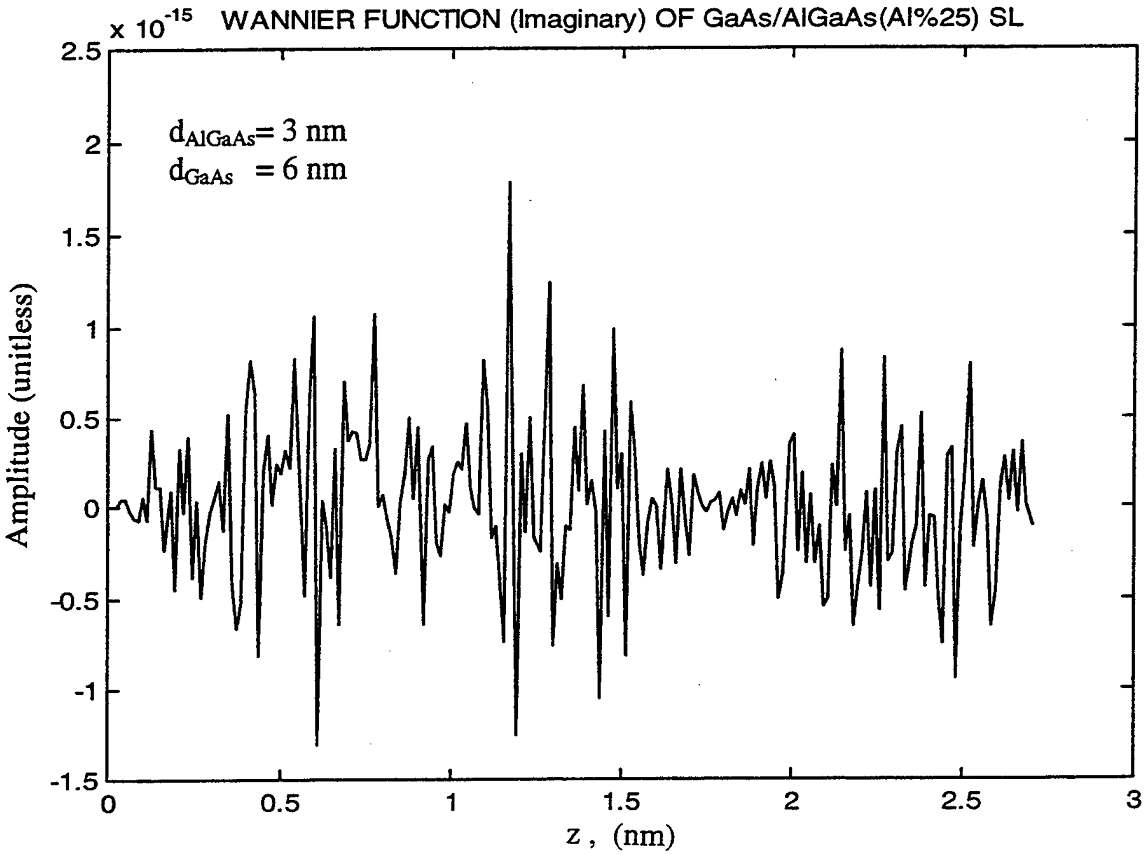

Figure 7: Imaginary part of the numerically calculated Wannier function of GaAs/$Al_{0.25}$ $Ga_{0.75}$ As superlattice for the first band index (n=2).

C. CONCLUSION AND FINAL REMARKS

In this thesis, we have developed an algorithm to numerically calculate the Wannier functions of a GaAs/$Al_{0.25}$ $Ga_{0.75}$ As superlattice structure. The algorithm has been built in two seperate steps : First we wanted to show the credibility of our numerical modelling of the superlattice effective-mass Schrodinger equation (Eqn. 27). We did that by comparing the bandstructure function modelled by our method with the one obtained by using the G. Bastard's superlattice dispersion relation (Appendix A). We proved that our modelling with the finite difference form is a very good approximation for the discretization of the superlattice effective-mass Schrodinger equation (Figures 2 and 3). In the next step, after confirming that our numerical modelling is reliable, we created a routine (Appendix B) for solving the eigenvalue matrix equation (Eqn. 32) for the Wannier functions of the GaAs/$Al_{0.25}Ga_{0.75}As$.

The results we obtained are in good agreement with the theory of the Wannier functions which we have discussed in detail in Chapter II. Although, in the past there were no attempts to calculate these functions for bulk crystals, we have demonstrated that the Wannier functions can be calculated even for a complex superlattice structure. By plotting the numerical simulation of the Wannier functions for the first couple of allowed bands (n=1 and n=2) of the superlattice structure , we displayed the peculiar properties of these functions:

a. Wannier functions are real (Figures 5 and 7).

b. They fall off exponentially (Figures 4 and 6).

c. They are either symmetric or anti-symmetric about z=0 (Figures 4 and 6).

Even though the results we reach conform with the theory, the numerical approach we have utilized create two shortcomings that we have to deal with. The first one which we pointed out before is the normalization problem of the Bloch functions. Since for every band index n and for each value of k there is a Bloch state ($\psi_{nk}(z)$), normalization for a continuous k values is a formidable task to do, e.g., just for the first band, the computer code in Appendix B has simulated 16800 Bloch functions for discrete values of k. Besides, we have to note that we just extend the Wannier functions to the next two superlattice sites to show the asymptotic behavior. But, as we have stated before, for the purpose of this paper it is unnecessary to normalize the Bloch states. The second problem we encounter is about the effective masses. In order to show all the aspects of the Wannier functions we have had to use a uniform effective mass throughout the simulation distance. The reason for that is the same as the first one: We could not discretize the superlattice site small enough to show the kink at each interface the Wannier functions should have had that would be due to the different effective masses at the interface. We used the smallest mesh distance that we could, but all we obtained was discontinuities at the interfaces.

Finally, we want to call attention to some of the future studies that we think will support the theory of the Wannier functions:

a. We have used Bloch states in the eigenvalue matrix equation to obtain the bandstructure function of the GaAs/$Al_{0.25}Ga_{0.75}As$ superlattice structure. An algorithm can be developed to use the Wannier functions in the calculation of the energy bandstructure functions of the superlattices.

b. $Al_xGa_{1-x}As$ bulk alloy is a direct-bandgap semiconductor if $x<0.45$ [Ref. 26] There is a crossover from direct to indirect-bandgap structure at about $x=0.45$. The Wannier functions of such a structure can be studied in the future.

c. The GaAs/$Al_{0.25}Ga_{0.75}As$ superlattice structure is a type 1 superlattice. The Wannier functions of type 2 and type 3 superlattices can be studied in the future.

d. If Wannier functions of all types of superlattice structures are obtained, maybe an electronic transport theory can be developed based on the Wannier functions.

APPENDIX A: COMPUTER CODE IN MATLAB PROGRAMMING LANGUAGE FOR NUMERICAL CALCULATION OF THE BANDSTRUCTURE FUNCTION

```
format long g

%%%%%%%%%%%%%%%%%%%%%%%%%%%%%%%%%%%%%%%%%%%%%%%%%%%%%%%%%%%%%%%%%%%%%
%%%%%%%%%%%%%%%%%%%%%%%   INPUT PARAMETERS  %%%%%%%%%%%%%%%%%%%%%%%%%
%%%%%%%%%%%%%%%%%%%%%%%%%%%%%%%%%%%%%%%%%%%%%%%%%%%%%%%%%%%%%%%%%%%%%

          EgG=input('Energy gap for GaAs (eV)');
          hh=input('barier thickness (nm)');
          LL=input('well thickness   (nm)');
          x=input('Al concentration (x)');

%%%%%%%%%%%%%%%%%%%%%%%%%%%%%%%%%%%%%%%%%%%%%%%%%%%%%%%%%%
%%%%%%%%%%%%%%%  DEFINING THE CONSTANTS  %%%%%%%%%%%%%%%%%
%%%%%%%%%%%%%%%%%%%%%%%%%%%%%%%%%%%%%%%%%%%%%%%%%%%%%%%%%%

             hbar=6.5821e-16;
             m1=0.067;
             me=(0.511e6)/9e16;
             m2= (m1+0.0838*x);
             EgA=EgG+1.247*x;
             Ec=(0.65*(EgA-EgG)); %CONDUCTION BAND OFFSET

             h=hh/1000000000;
             L=LL/1000000000;
             d=h+L;
             D=(h/2)+L;
             s=3.14/d;
             in=100;
             dz=d/in;
             dq=floor(s/50);
             w=-(hbar^2)/(2*me*(dz^2));


%%%%%%%%%%%%%%%%%%%%%%%%%%%%%%%%%%%%%%%%%%%%%%%%%%%%%%%%%%
%%%%%%%%%%%%%%%%%%%%%  HAMILTONIAN (H ) %%%%%%%%%%%%%%%%%%
%%%%%%%%%%%%%%%%%%%%%%%%%%%%%%%%%%%%%%%%%%%%%%%%%%%%%%%%%%

for l=1:in
    z(l)=dz*l;
  if z(l)>h/2 & z(l)<D
      V(l)=0;
      HH(l)=V(l)-(2/m1)*w;
      m(l)=m1;
      Ww(l)=w/m1;
 else
      V(l)=Ec;
      HH(l)=V(l)-(2/m2)*w;
      Ww(l)=w/m2;
 end
end

Ww(floor(in/6))=(2*w)/(m1+m2);Ww(floor(in*5/6))=(2*w)/(m1+m2);

HH1=diag(HH);
W=Ww(1:(length(Ww)-1));
W1=diag(W,1);
```

```
W2=diag(W,-1);
HH2=(HH1+W1+W2);

%%%%%%%%%%%%%%%%%%%%%%%%%%%%%%%%%%%%%%%%%%%%%%%%%%%%%%%%
%%%%%%%%%%%%%%%%  FIRST BROULINE ZONE (BZ) %%%%%%%%%%%%%
%%%%%%%%%%%%%%%%%%%%%%%%%%%%%%%%%%%%%%%%%%%%%%%%%%%%%%%%

  for k=1:50;

            q1(k)=(k)*dq;
            Q1=(w/m2)*(cos(q1(k)*d)-i*sin(q1(k)*d));
            Q2=(w/m2)*(cos(q1(k)*d)+i*sin(q1(k)*d));
            Q11=diag(Q1,(in-1));Q22=diag(Q2,-(in-1));

            H=(HH2+Q11+Q22);   % HAMILTONIAN WITH BOUNDARY CONDITIONS

            kk=eig(H);         % ENERGY EIGENVALUES
            ee=sort(kk);

            EE1(k)=ee(1);      % BAND INDEX n=1
            EE2(k)=ee(2);      % BAND INDEX n=2
            EE3(k)=ee(3);      % BAND INDEX n=3

end
          qq1=-1*fliplr(q1);
          q=[qq1 q1];

               EE11=fliplr(EE1);E1=[EE11 EE1];

               EE22=fliplr(EE2); E2=[EE22 EE2];

               EE33=fliplr(EE3);E3=[EE33 EE3];

  %%%%%%%%%%%%%%%%%%%%%%%%%%%%%%%%%%%%%%%%%%%%%%%%%%%%%%%
  %%%%%%% PLOTTING BANDSTRUCTURE FUNCTION %%%%%%%%%%%%%%%
  %%%%%%% WITH EIGENVALUE MATRIX EQUATION %%%%%%%%%%%%%%%
  %%%%%%%%%%%%%%%%%%%%%%%%%%%%%%%%%%%%%%%%%%%%%%%%%%%%%%%
  figure(1),plot(q,E1,'k',q,E2,'k',q,E3,'k');
  axis([-s s 0 .45])
  title('BANDSTRUCTURE OF GaAs/AlGaAs(Al%25) SUPERLATTICE')
  xlabel('k (first BZ), 1/m')
  ylabel('Energy, eV')


%%%%%%%%%%%%%%%%%%%%%%%%%%%%%%%%%%%%%%%%%%%%%%%%%%%%%%%
%%%%%%%%%%%%%%%%%%%%%%%%%%%%%%%%%%%%%%%%%%%%%%%%%%%%%%%

%%%%%%%%%%%%%%%%%%%%%%%%%%%%%%%%%%%%%%%%%%%%%%%%%%%%%%%
%%%%%%%%  G. BASTARD'S DISPERSION RELATION %%%%%%%%%%%%
%%%%%%%%%%%%%%%%%%%%%%%%%%%%%%%%%%%%%%%%%%%%%%%%%%%%%%%

            mm1=m1*(0.511e6)/9e16;
            mm2=(m1+0.0838*x)*(0.511e6)/9e16;

            w1=sqrt(2*mm1)/hbar;
            w2=sqrt(2*mm2)/hbar;

            dq=1000000;
            dE=0.000002;

            d=h+L;dz=d/600;D=h/2+L;
            it=ceil(s/dq);
%%%%%%%%%%%%%%%%%%%%%%%%%%%%%%%%%%%%%%%%%%%%%%%%%%%%%%%%
```

```
%%%%%%%%%%%%%%%%%   DISPERSION RELATION    %%%%%%%%%%%%
%%%%%%%%%%%%%%%%%%%%%%%%%%%%%%%%%%%%%%%%%%%%%%%%%%%%%%

   n=1:1:200000;
   E=.05+n.*dE;
      p1=(cos((sqrt(E)).*w1*L)).*(cosh((sqrt(Ec-E)).*w2*h));
      p2=1/2*((-sqrt((Ec-E)./E).*sqrt(m2/m1))+(1./(sqrt((Ec-
E)./E).*sqrt(m2/m1))));
      p3=(sin((sqrt(E)).*w1*L)).*(sinh((sqrt(Ec-E)).*w2*h));
      p=p1-p2.*p3;

%%%%%%%%%%%%%%%%%%%%%%%%%%%%%%%%%%%%%%%%%%%%%%%%%%%%%%%
%%%%%%%%%%%%%%%%  FIRST BROULINE ZONE (BZ) %%%%%%%%%%%%
%%%%%%%%%%%%%%%%%%%%%%%%%%%%%%%%%%%%%%%%%%%%%%%%%%%%%%

   for v=1:it
       q=v*dq;
       g(v)=cos(q*d);
       [yy hh]=min(abs(g(v)-p));
       Ee(v)=.05+hh*dE;
       qq(v)=q;
   end
ff=(-1)*fliplr(qq);
k=[ff qq];             % FIRST BRUOILLOIN ZONE
ee=fliplr(Ee);
EE=[ee Ee];            %  E(k)

figure(2),plot(k,EE,'b.')
axis([-s s 0 0.45])
title(['BANDSTRUCTURE OF GaAs/AlGaAs(x=.25) SUPERLATTICE (Bastard)'])
xlabel('k (first BZ), 1/m')
ylabel('Energy (eV)')
```

APPENDIX B: COMPUTER CODE IN MATLAB PROGRAMMING LANGUAGE FOR NUMERICAL CALCULATION OF THE WANNIER FUNCTIONS

```
format long g

%%%%%%%%%%%%%%%%%%%%%%%%%%%%%%%%%%%%%%%%%%%%%%%%%%%%%%%%%%%%%%%%%%%%%
%%%%%%%%%%%%%%%%%%%%%%%   INPUT PARAMETERS   %%%%%%%%%%%%%%%%%%%%%%%%
%%%%%%%%%%%%%%%%%%%%%%%%%%%%%%%%%%%%%%%%%%%%%%%%%%%%%%%%%%%%%%%%%%%%%

            EgG=input('Energy gap for GaAs (eV)');
            hh=input('barier thickness (nm)');
            LL=input('well thickness   (nm)');
            x=input('Al concentration (x)');

%%%%%%%%%%%%%%%%%%%%%%%%%%%%%%%%%%%%%%%%%%%%%%%%%%%%%%%%%%%%%%%%%%%%%
%%%%%%%%%%%%%%%%%%  DEFINING THE CONSTATNTS  %%%%%%%%%%%%%%%%%%%%%%%%
%%%%%%%%%%%%%%%%%%%%%%%%%%%%%%%%%%%%%%%%%%%%%%%%%%%%%%%%%%%%%%%%%%%%%

            hbar=6.5821e-16;
            m1=0.067;
            me=(0.511e6)/9e16;
            m2= (m1+0.0836*x);

            EgA=EgG+1.247*x;             %AlGaAs bandgap for given(x)
            Ec=(0.65*(EgA-EgG));         %Conduction band offset

            h=hh/1000000000;
            L=LL/1000000000;
            d=(h)+L;
            D=(h/2)+L; DH=D+h; DHL=DH+L ;DHLH=DHL+(h); DHLHL=DHLH+L;
            s=3.14/d;
            ind=210;
            dz=d/70;
            inq=40;
            dq=floor(s/inq);
            w=-(hbar^2)/(2*me*(dz^2));

%%%%%%%%%%%%%%%%%%%%%%%%%%%%%%%%%%%%%%%%%%%%%%%%%%%%%%%%%%%%%%%%%%%%%
%%%%%%%%%%%%%%%%%%%%%     HAMILTONIAN (H)    %%%%%%%%%%%%%%%%%%%%%%%%
%%%%%%%%%%%%%%%%%%%%%%%%%%%%%%%%%%%%%%%%%%%%%%%%%%%%%%%%%%%%%%%%%%%%%


for l=1:ind
    z(l)=dz*l;
  if z(l)>(h/2) & z(l)<D
      V(l)=0;
      HH(l)=V(l)-(2/m1)*w;
      m(l)=m1;
      Ww(l)=w/m1;
elseif z(l)>D &z(l)<DH
      V(l)=Ec;
      HH(l)=V(l)-(2/m1)*w;
      Ww(l)=w/m1;
   elseif z(l)>DH & z(l)<DHL
      V(l)=0;
      HH(l)=V(l)-(2/m1)*w;
      m(l)=m1;
      Ww(l)=w/m1;
   elseif   z(1)>DHL & z(1)<DHLH
      V(1)=Ec;
      HH(1)=V(1)-(2/m1)*w;
      Ww(1)=w/m1;
   elseif z(1)>DHLH &  z(1)<DHLHL
     V(1)=0;
     HH(1)=V(1)-(2/m1)*w;
     m(1)=m1;
     Ww(1)=w/m1;
  else %z(1)>DLHL %& z(1)<DLHLD
     V(1)=Ec;
      HH(1)=V(1)-(2/m1)*w;
      Ww(1)=w/m1;
   end
end

%Ww(floor(ind/18))=(2*w)/(m1+m2);
%Ww(floor(ind*7/18))=(2*w)/(m1+m2);
%Ww(floor(ind*11/18))=(2*w)/(m1+m2);
%Ww(floor(ind*13/18))=(2*w)/(m1+m2);
%Ww(floor(ind*17/18))=(2*w)/(m1+m2);


HH1=diag(HH);
W=Ww(1:(length(Ww)-1));
W1=diag(W,1);
W2=diag(W,-1);

HH2=(HH1+W1+W2);

n1=zeros(ind,1);n2=zeros(ind,1);n3=zeros(ind,1);

  for k=1:2*inq;
     if k>inq
        q1(k-inq)=(k-inq)*dq;
        Q1=(w/m1)*(cos(q1(k-inq)*d)-i*sin(q1(k-inq)*d));
        Q2=(w/m1)*(cos(q1(k-inq)*d)+i*sin(q1(k-inq)*d));
    else
     q1(k)=-k*dq;
     Q1=(w/m1)*(cos(q1(k)*d)-i*sin(q1(k)*d));
     Q2=(w/m1)*(cos(q1(k)*d)+i*sin(q1(k)*d));
    end
     Q11=diag(Q1,(ind-1));Q22=diag(Q2,-(ind-1));

     H=(HH2+Q11+Q22);
     [jj kk]=eig(H);
     ee=sort(diag(kk));
     [f1 g1]=find(ee(1)==kk);
     [f2 g2]=find(ee(2)==kk);
     [f3 g3]=find(ee(3)==kk);

     n1=n1+(jj(:,f1));
     n2=n2+(jj(:,f2));
 end

%%%%%%%%%%%%%%%%%%%%%%%%%%%%%%%%%%%%%%%%%%%%%%%%%%%%%%%%%%%%%%%%%%%%%%
%%%%%%%%%%%%%% PLOTTING OF THE WANNIER FUNCTIONS  %%%%%%%%%%%%%%%%%%%%
%%%%%%%%%%%%%%%%%%%%%%%%%%%%%%%%%%%%%%%%%%%%%%%%%%%%%%%%%%%%%%%%%%%%%%

 g=1:ind;
 figure(1),plot((g.*dz).*100000000,n1,'k')
 title('WANNIER FUNCTION OF GaAs/AlGaAs(Al%25) SUPERLATTICE')
 xlabel('z , nm ')
```

```
ylabel('Amplitude (arbitrary)')

figure(2),plot((g.*dz).*100000000,n2,'k')
title('WANNIER FUNCTION OF GaAs/AlGaAs(Al%25) SUPERLATTICE ')
xlabel('z , nm  ')
ylabel('Amplitude (arbitrary)')
```

LIST OF REFERENCES

1. Kelly, M. J., *Low Dimensional Semiconductors*, p. 266, Oxford Science Publications, 1995.
2. Esaki, L., *Proc. 17th Int. Conf. Physics of Semiconductors*, p.473, ed. D.J. Chadi and W.A. Harrison, Springer-Verlag, 1984.
3. Taguchi, K., Makita, K., Watanabe, I., Tsuji, M., Hayashi, M., Nakata, T., *Optical and Quantum Electronics*, 30, p.219, 1998.
4. Manasreh, M.O., Brown, G.J., *Semiconductor Quantum Wells and Superlattices for Long-Wavelength Infrared Detectors*, p.2-5, ed. Manasreh, M.O., Artech House, 1993.
5. Dingle, R., Wiegman, C.H., Henry, C.H., *Phys. Rev. Lett.* **33**, p.827, 1974.
6. Wainright, T., Parzen, G., *Phys. Rev.* **92**, p.1129, 1953.
7. Cohen, M., *Intro. to the Quantum Theory of Semiconductors*, p.179, Gordon and Breach Science Publishers, 1972.
8. Bloch, F., Zeit. Physik, **52**, p.555, 1928.
9. Ashcrot, N., Mermin, D., *Solid State Physics*, p.179, Saunders College Publications,1976.
10. Wannier, G., *Phys. Rev.*, **52**, p.191, 1937.
11. Kohn, W., *Phys. Rev.*, **115**, p.816, 1959.
12. Kohn, W., *Phys. Rev.*, **115**, p.819, 1959.
13. Ashcrot, N., Mermin, D., *Solid State Physics*, p.188, Saunders College Publications,1976.
14. Koster, G. F., *Phys. Rev.*, **89**, p.67, 1952.
15. L., Pincherle, *Electronic Energy Bands in Solids*, p.39-46, Macdonald, 1971.
16. Merzbacher, E., *Quantum Mechanics*, p.139-141, John Wiley&sons, 1961.
17. Haug, A., *Theoretical Solid State Physics Vol.1*, p.113-114, Pergamon Press.

18. Bastard, G., *Wave Mechanics Applied to Semiconductor Heterostructures*, p.36-50, Halsted Press, 1988.

19. Nag, B.R., *Electron Transport in Compound Semiconductors*, p.26-30, Springer-Verlag, 1980.

20. Bastard, G., *Wave Mechanics Applied to Semiconductor Heterostructures*, p.36-50, Halsted Press, 1988.

21. Jasprit, S., *Physics of Semiconductors and Their Heterostructures*, p.185-189, Mcgraw-Hill, 1993.

22. Giordano, N., *Computational Physics*, p.114, Prentice Hall, 1997.

23. Manasreh, M.O., Brown, G.J., *Semiconductor Quantum Wells and Superlattices for Long-Wavelength Infrared Detectors*, p.27, ed. Manasreh, M.O., Artech House, 1993.

24. Bastard, G., *Wave Mechanics Applied to Semiconductor Heterostructures*, p.20-21, Halsted Press, 1988.

25. Kohn, W., *Phys. Rev.*, **115**, p.818-820, 1959.

26. Kelly, M. J., *Low Dimensional Semiconductors*, p.19-20, Oxford Science Publications, 1995.

INITIAL DISTRIBUTION LIST

1. Defense Technical Information Center 2
   8725 John J. Kingman Rd., STE 0944
   Ft. Belvoir, VA 22060-6218

2. Dudley Knox Library 2
   Naval Postgraduate School
   411 Dyer Rd.
   Monterey, CA 93943-5101

3. Professor J. H. Luscombe 1
   Code PH/Lj
   Naval Postgraduate School
   Monterey, CA 93943-5002

4. Professor Robert L. Armstead 1
   Code PH/Ar
   Naval Postgraduate School
   Monterey, CA 93943-5002

5. Kara Kuvvetleri Komutanligi 1
   Personel Daire Baskanligi
   Bakanliklar, Ankara
   Turkey

6. Kara Harp Okulu Komutanligi 1
   Kutuphane
   06654 Bakanliklar, Ankara
   Turkey

7. Mustafa Yuvanc 1
   337 Sokak, No: 92/4
   Sirinyer, IZMIR
   Turkey

8. Ortadogu Teknik Universitesi Kutuphanesi 1
   Balgat, Ankara
   Turkey

9. Bilkent Universitesi Kutuphanesi 1
   Bilkent, Ankara
   Turkey

10. K.K.K. Egitim ve Doktrin Komutanligi 1
Muharebe Lab.
Balgat, Ankara
Turkey

11. Engineering and Technology Curriculum Code 34 1
Naval Postgraduate School
700 Dyer Road, Room 115
Monterey, CA 93943-5107